Zurich Open Repository and Archive
University of Zurich
University Library
Strickhofstrasse 39
CH-8057 Zurich
www.zora.uzh.ch

Year: 2019

Nicotinamide Riboside Derivatives: Single Crystal Growth and Determination of X-ray Structures

Alvarez, Ricardo ; Schabert, Günter ; Soydemir, Aysel ; Wick, Lukas ; Spitz, Urs ; Spingler, Bernhard

Abstract: For the first time, the X-ray structure of nicotinamide riboside could be determined. Five nicotinamide riboside (NR) derivatives in their native, thioamide and triacetyl protected form could be crystallized as their chloride and bromide salts. The single crystals were obtained with the help of the vapor diffusion technique. The use of the much slower layering technique for crystallization led to the decomposition of the nicotinamide ribosides yielding the corresponding nicotinamide salts. The torsion angles of the five nicotinamide riboside derivatives were compared with those obtained from the two nicotinamide adenine dinucleotide crystal and the three protein nicotinamide riboside cocrystal structures.

DOI: https://doi.org/10.1021/acs.cgd.9b00423

Posted at the Zurich Open Repository and Archive, University of Zurich
ZORA URL: https://doi.org/10.5167/uzh-171652
Journal Article
Accepted Version

Originally published at:
Alvarez, Ricardo; Schabert, Günter; Soydemir, Aysel; Wick, Lukas; Spitz, Urs; Spingler, Bernhard (2019). Nicotinamide Riboside Derivatives: Single Crystal Growth and Determination of X-ray Structures. Crystal Growth Design, 19(7):4019-4028.
DOI: https://doi.org/10.1021/acs.cgd.9b00423

Nicotinamide Riboside Derivatives: Single Crystal Growth and Determination of X-ray Structures

Ricardo Alvarez[1], Günter Schabert[2], Aysel Soydemir[2], Lukas Wick[2], Urs Spitz[2], Bernhard Spingler[1*]

[1] Department of Chemistry, University of Zurich, 8057 Zurich, Switzerland

[2] BIOSYNTH AG, Rietlistrasse 4, 9422 Staad, Switzerland

[*] Corresponding author: spingler@chem.uzh.ch

Abstract

For the first time, the X-ray structure of nicotinamide riboside could be determined. Five nicotinamide riboside (NR) derivatives in their native, thioamide and triacetyl protected form could be crystallized as their chloride and bromide salts. The single crystals were obtained with the help of the vapour diffusion technique. The use of the much slower layering technique for crystallization led to the decomposition of the nicotinamide ribosides yielding the corresponding nicotinamide salts. The χ torsion angles of the five nicotinamide riboside derivatives were compared with those obtained from the two NAD crystal and the three protein nicotinamide riboside co-crystal structures.

1. Introduction

Nicotinamide riboside (NR) is a naturally occurring nucleoside present in almost all living organisms. Even though the metabolic pathway of NR has yet to be fully understood, recent studies imply that NR is a potent nicotinamide adenine dinucleotide (NAD^+) precursor[1-3] and an additional vitamin B3 form.[4] The discovery of nicotinamide riboside kinases (NRK 1 and 2) in humans implied that an NRK-dependent pathway should exist in humans.[5] This hypothesis was proven to be correct for mammalian cells in 2016.[1] Yang *et al*. showed that NR treated cells have a 270% increase in NAD^+ production compared to control experiments.[6] This implied a greater potency of NR than nicotinamide or nicotinic acid as neither of them have been able to induce such high levels of NAD^+. NR is a promising candidate for the treatment of several conditions including metabolic and neurodegenerative diseases and has received the GRAS (generally recognised as safe) status from FDA. Therefore it can be consumed as a food supplement.[7] A recent study showed that permanent supply of nicotinamide riboside increases the NAD^+ level in middle age to elderly persons.[8] Finally, the concentration of NR in cow milk was found to be at lower μM levels.[9] In a recent patent, a crystalline form of nicotinamide ribose chloride was described to have advantageous properties relative to amorphous forms, e.g. since it may be better purified compared to amorphous forms.[10] The crystalline chloride salt was obtained from an amorphous chloride salt by re-crystallization in a polar solvent such as methanol. We were surprised to see that not a single crystal structure of NR and of its derivatives that are not phosphate esters has been reported so far. Therefore, we started a study in order to determine the X-ray structures of the five NR derivatives shown in Figure 1.

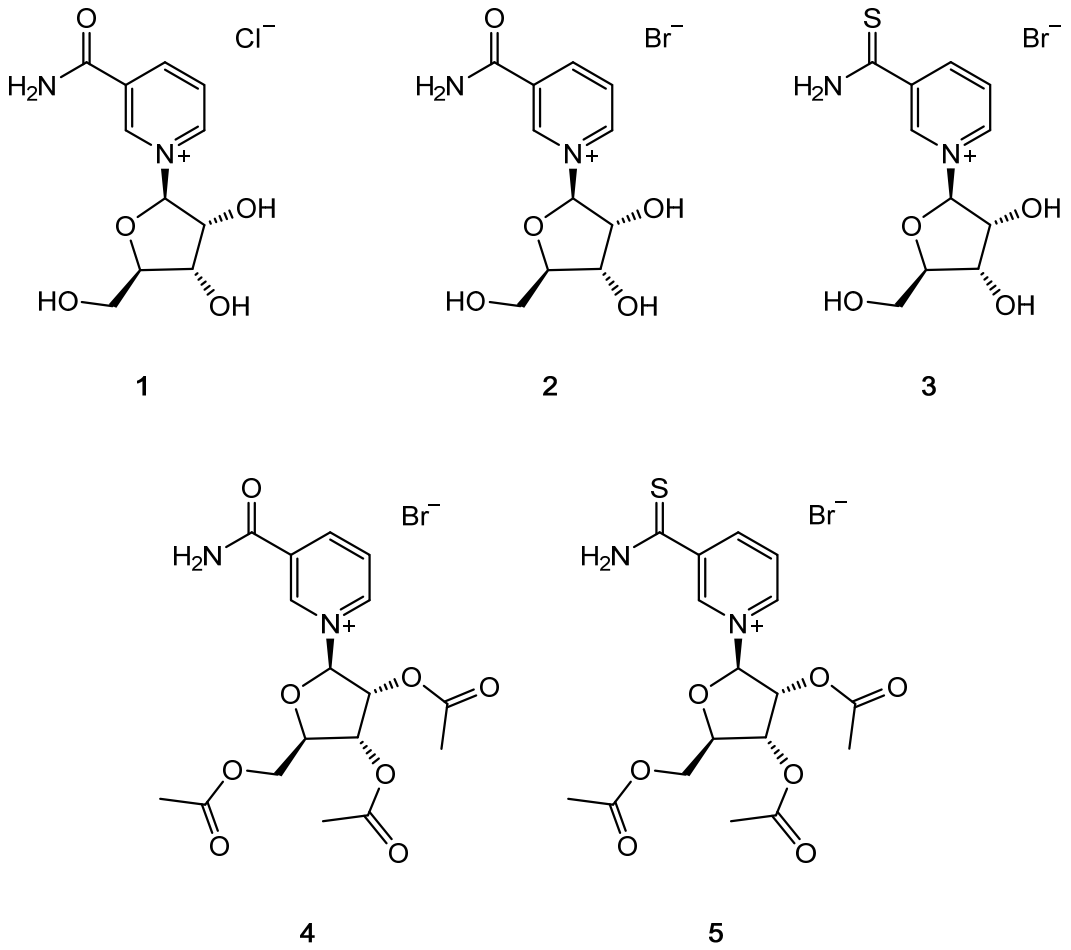

Figure 1: The tested nicotinamide derivatives: nicotinamide-β-D-riboside chloride (**1**), nicotinamide-β-D-riboside bromide (**2**), thionicotinamide-β-D-riboside bromide (**3**), nicotinamide-β-D-riboside triacetate bromide (**4**), and thionicotinamide-β-D-riboside triacetate bromide (**5**).

2. **Results & Discussion**

Initial crystallization attempts employed the layering technique, in which the compound of interest is dissolved in one dense solvent, placed in a narrow tube (normally an NMR tube). The solution is then carefully covered by a less dense anti-solvent. While this technique is known to produce nice crystals, it takes weeks until the mixing of the solvent and the anti-solvent results in the growth of single crystals.[11] Initial crystallization attempts of nicotinamide ribose salts employing the layering technique with ethanol or methanol as solvents and isopropanol or tetrahydrofuran as anti-solvents yielded exclusively the corresponding protonated nicotinamide as a salt. These results can easily be explained by the well known instability of nicotinamide ribose salts. Oppenheimer determined the pH independent first order hydrolysis rate of nicotinamide ribose at 25°C as $k = 10^{-5.8}/s$.[12] Assuming that the layering experiment takes at least

2 weeks and inserting the above value of k into the equation E1, one can calculate that after this time already 85% of the nicotinamide ribose have been hydrolysed to give the nicotinamide. Therefore we decided to next employ the vapour diffusion technique, which can yield crystals as fast as within 15 hours.[11]

E1 $[A] = [A_o]e^{-kt}$

2.1 Nicotinamide-β-D-riboside chloride (1)

Single crystals were obtained by vapour diffusion at 23°C of 4 mg of **1** dissolved in ethanol against a reservoir of cyclohexane. The crystallographic data is summarised in Table 1. **1** crystallised in the orthorhombic, chiral space group $P2_12_12_1$. The asymmetric unit consists of one molecule of **1** (Figure 2). The absolute configuration of the enantiomerically pure molecule was confirmed by the Flack parameter (-0.004(6)) and by comparison with the expected stereochemistry. The nitrogen of the amide group forms a hydrogen bond to the oxygen of a neighbouring amide group and another one to the chloride (N2-H2B O1(-0.5+x, -0.5-y, 1-z): 2.912(3) Å, N2-H2A Cl1(x, -1+y, z): 3.3359(19) Å). The alcohol groups of the riboside form hydrogen bonds to neighbouring alcohol groups and from the alcohol at C5 to the chloride (O2-H2 O3(2-x, -0.5+y, 1.5-z): 2.7024(19) Å, O3-H3 O5(1-x, -0.5+y, 1.5-z): 2.6792(18) Å, O5-H5 Cl1: 3.0459(16) Å). Crystalline material, which was obtained by vapour diffusion of **1** dissolved in methanol against a reservoir of tetrahydrofuran, crystallised in the same space group $P2_12_12_1$ but was not suitable for single crystal X-ray analysis due to multiple twinning.

a)

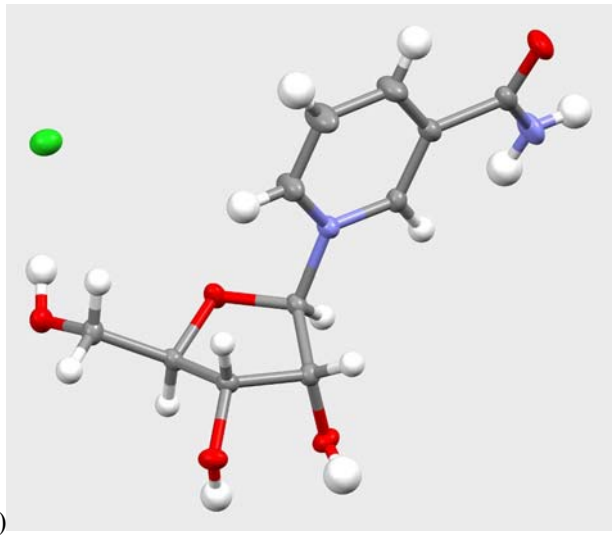

b) 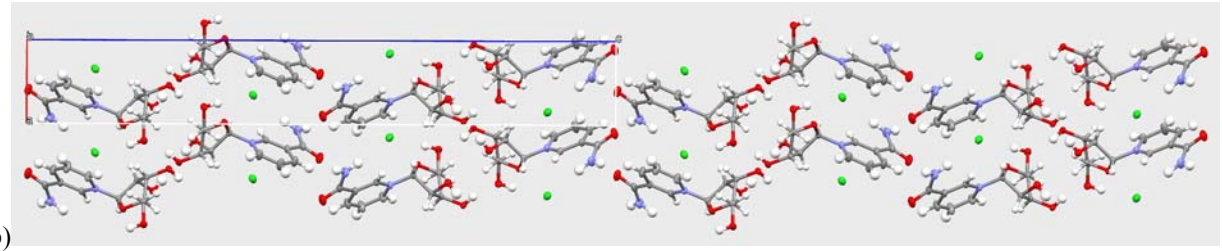

Figure 2: a) Displacement ellipsoid representation of **1**, ellipsoids drawn at 50% probability. b) packing diagram of **1**.

Two patents for crystalline nicotinamide riboside chloride (**1**) were found, WO2016014927A2[10] from *W.R. Grace & Co.-Conn.* and WO2015186068A1[13] from *GlaxoSmithKline*, both filed in 2015. In both cases, the crystalline nicotinamide riboside chloride was characterised by powder X-ray diffraction (PXRD). In Figure 3 (top) the published PXRD pattern from patent WO2016014927A2 is shown. It looks very similar to the simulated PXRD pattern of **1** (Figure 3, bottom), thus indicating that it is indeed the same crystal structure.

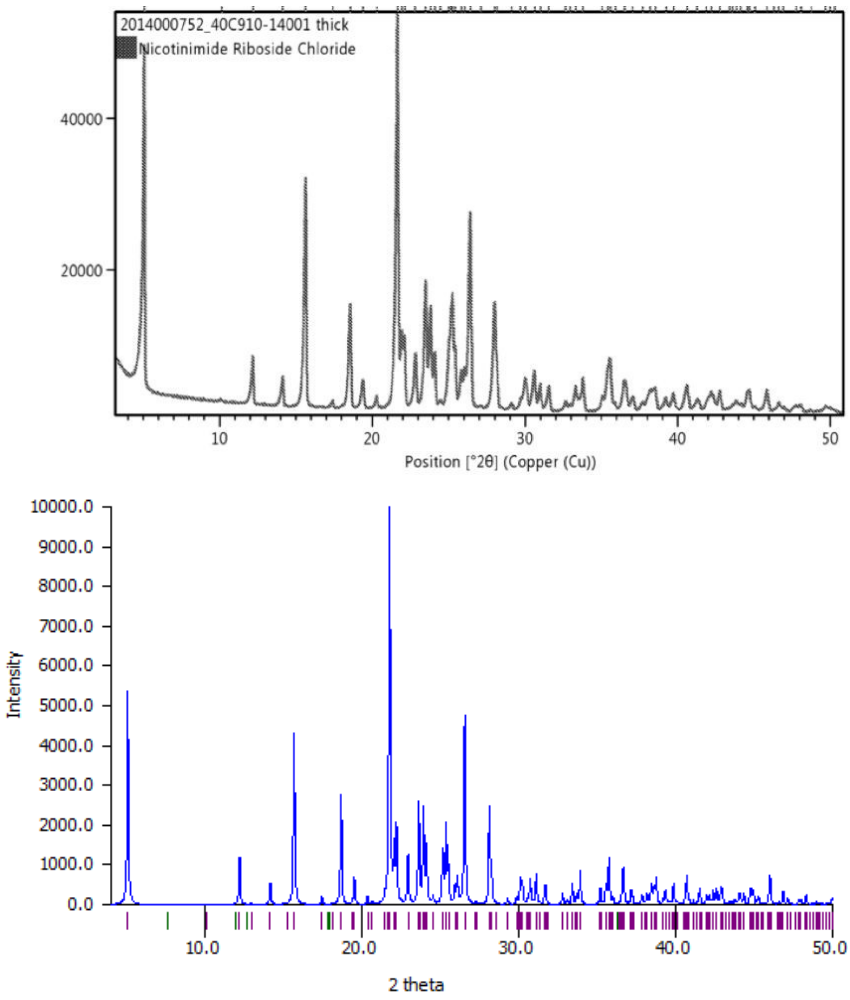

Figure 3: Top: Published PXRD pattern of solvate free **1** from patent WO2016014927A2.[10] Bottom: PXRD pattern of **1** simulated from single crystal data.

The published PXRD pattern of **1** from patent WO2015186068A1 is shown in Figure 4. It looks not as similar compared to the simulated PXRD pattern (Figure 3, bottom) as the pattern from patent WO2016014927A2. The peaks are slightly shifted to lower 2θ angles and differences occur in the 2θ range of 30° to 40°. As described in the patent the crystalline material was obtained from drying nicotinamide riboside chloride·0.9 methanol crystals under high vacuum and at ambient temperature for 48 h. Therefore, traces of the solvate methanol (MeOH) could still be present which could be responsible for the differences in the PXRD pattern. Furthermore, this patent contains a PXRD pattern of nicotinamide riboside chloride·0.9 methanol with negative diffraction angles, which is physically impossible.

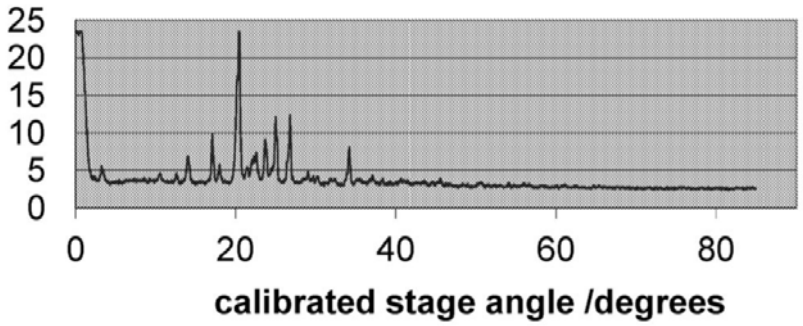

Figure 4: Published PXRD pattern of **1** with only trace amount of MeOH solvent from patent WO2015186068A1.[13]

2.2 Nicotinamide-β-D-riboside bromide (2)

Single crystals were obtained by vapour diffusion at 23°C of 4 mg of **2** dissolved in methanol against a reservoir of tetrahydrofuran. The crystallographic data is summarised in Table 1. **2** crystallised in the orthorhombic, chiral space group $P2_12_12_1$. The asymmetric unit consists of one molecule of **2** (Figure 5). The structure is essentially isostructural with the chloride salt **1**. The absolute configuration of the enantiomerically pure molecule was confirmed by the Flack parameter (0.012(4)) and by comparison with the expected stereochemistry. The nitrogen of the amide group forms a hydrogen bond to the oxygen of a neighbouring amide group and another one to the bromide (N2-H2B O1(0.5+x,-0.5-y,1-z): 2.916(4) Å, N2-H2A Br1(x,-1+y,z): 3.476(3) Å). The alcohol groups of the riboside form hydrogen bonds to neighbouring alcohol groups and from the alcohol at C5 to the bromide (O2-H2 O3(-x, -0.5+y, 0.5-z): 2.744(3) Å, O3-H3 O5(1-x, -0.5+y, 0.5-z): 2.663(3) Å, O5-H5 Br1: 3.194(2) Å).

a)

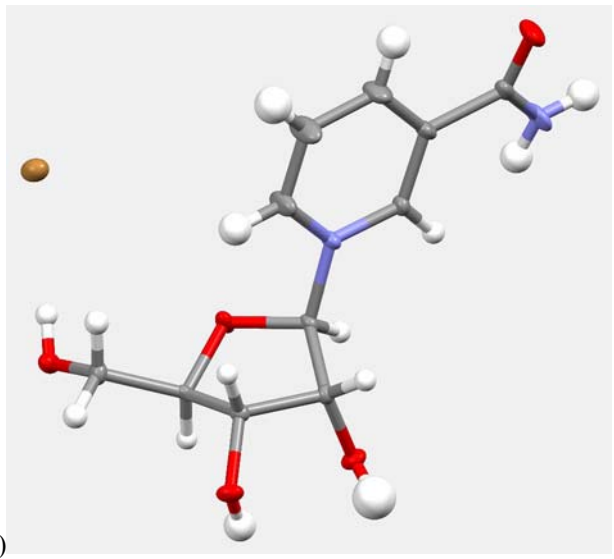

b)

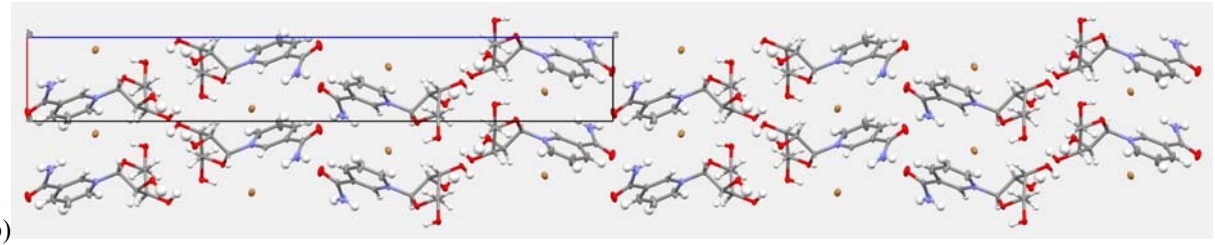

Figure 5: a) Displacement ellipsoid representation of **2**, ellipsoids drawn at 50% probability. b) packing diagram of **2**.

2.3 Thionicotinamide-β-D-riboside bromide (3)

Single crystals were obtained by vapour diffusion at 23°C of 4 mg of **3** dissolved in methanol against a reservoir of tetrahydrofuran. The crystallographic data is summarised in Table 1. **3** crystallised in the orthorhombic, chiral space group $P2_12_12_1$. The asymmetric unit consists of one molecule of **3** (Figure 6). The structure is essentially isostructural with the chloride and the bromide salts **1** and **2**. The absolute configuration of the enantiomerically pure molecule was confirmed by the Flack parameter (-0.011(10)) and by comparison with the expected stereochemistry. The nitrogen of the thioamide group forms a hydrogen bond to the sulfur of a neighbouring thioamide group and another one to the bromide (N2-H2B S1(-0.5+x,2.5-y,1-z): 3.428(3) Å, N2-H2A Br1(x,1+y,z): 3.461(3) Å). The alcohol groups of the riboside form hydrogen bonds to neighbouring alcohol groups and from the alcohol at C5 to the bromide (O2-H2 O3(2-x, -0.5+y, 1.5-z): 2.675(3) Å, O3-H3 O5(1-x, -0.5+y, 1.5-z): 2.742(3) Å, O5-H5 Br1: 3.201(2) Å).

a)

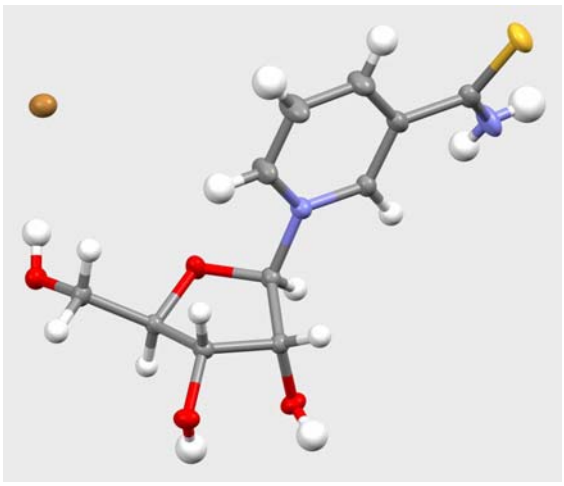

b)

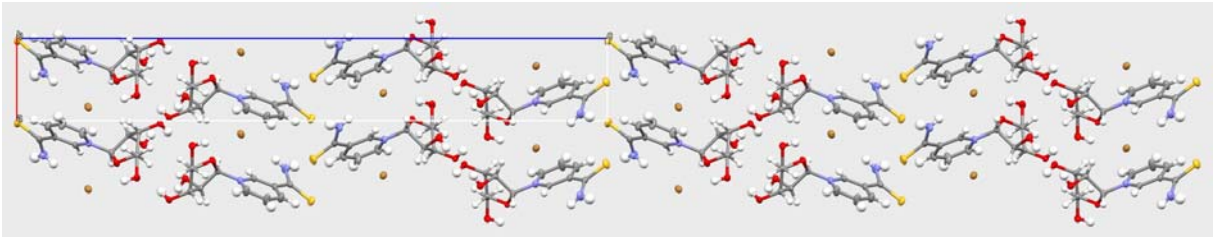

Figure 6: a) Displacement ellipsoid representation of **3**, ellipsoids drawn at 50% probability. b) packing diagram of **3**.

Table 1: Summary of crystal data and structure refinement of the isostructural salts **1**, **2** and **3**.

	1	**2**	**3**
Empirical formula	$[C_{11}H_{15}N_2O_5][Cl]$	$[C_{11}H_{15}N_2O_5][Br]$	$[C_{11}H_{15}N_2O_4S][Br]$
mol. weight [g/mol]	290.70	335.16	351.22
Crystal system	orthorhombic	orthorhombic	orthorhombic
Space group	$P2_12_12_1$	$P2_12_12_1$	$P2_12_12_1$
a [Å]	4.93730(10)	4.99710(10)	5.04050(10)
b [Å]	7.41700(10)	7.5323(2)	7.56260(10)
c [Å]	34.8797(5)	35.0875(10)	36.3551(5)
Volume [$Å^3$]	1277.29(4)	1320.68(6)	1385.83(4)
Z	4	4	4
Density(calc.) [mg/m^3]	1.512	1.686	1.683
Abs. coeff. [mm^{-1}]	2.851	3.131	5.580
F(000)	608	680	712

Crystal size [mm^3]	0.076 x 0.020 x 0.016	0.334 x 0.136 x 0.032	0.213 x 0.029 x 0.016
Crystal description	colourless needle	colourless plate	light yellow needle
Θ range [°]	5.072 to 78.782	2.322 to 32.934	4.866 to 78.463
Index ranges	-4≤h≤6, -8≤k≤9, -44≤l≤43	-7≤h≤7, -11≤k≤10, -49≤l≤52	-5≤h≤6, -9≤k≤6, -46≤l≤41
Reflections collected	11599	17105	12483
Indep. reflections	2755 [R_{int} = 0.0283]	4398 [R_{int} = 0.0393]	2989 [R_{int} = 0.0261]
Reflections obs.	2635	3986	2939
Criterion for obs.	I > 2σ(I)	I > 2σ(I)	I > 2σ(I)
Completeness to Θ [°]	99.9% to 67.684	99.9% to 25.242	99.9% to 67.684
Absorption correction	Gaussian	semi-empirical from equivalents	Gaussian
Max. and min. transmission	1.000 and 0.867	1.00000 and 0.74277	1.000 and 0.499
Data / restraints / parameters	2755 / 0 / 178	4398 / 0 / 184	2989 / 0 / 184
Goodness-of-fit on F^2	1.070	1.136	1.066
Final R indices	R_1 = 0.0237,	R_1 = 0.0360,	R_1 = 0.0220,
[$I > 2\sigma(I)$]	wR_2 = 0.0616	wR_2 = 0.0642	wR_2 = 0.0554
R indices (all data)	R_1 = 0.0250, wR_2 = 0.0622	R_1 = 0.0427, wR_2 = 0.0653	R_1 = 0.0225, wR_2 = 0.0556
Flack parameter	-0.005(6)	0.012(4)	-0.011(10)
Final $\Delta\rho_{max,min}$ [$e^-/Å^3$]	0.21 and -0.18	0.84 and -0.96	0.28 and -0.36

2.4 Nicotinamide-β-D-riboside triacetate bromide (4)

Single crystals were obtained by vapour diffusion at 23°C of 4 mg of **4** dissolved in ethanol against a reservoir of cyclohexane. The crystallographic data is summarised in Table 2. **4** crystallised in the monoclinic, chiral space group *C*2. The asymmetric unit consists of one molecule of **4** (Figure 7). The absolute configuration of the enantiomerically pure molecule was confirmed by the Flack parameter (-0.0038(18)) and by comparison with the expected stereochemistry. The nitrogen of the amide group forms two hydrogen bonds to two different bromide anions (N2-H2A Br1(0.5+x, 0.5+y, z): 3.4185(17) Å, N2-H2B Br1(1.5-x, 0.5+y, 2-z): 3.4051(15) Å). Crystalline material obtained by vapour diffusion of **4** dissolved in methanol against a reservoir of tetrahydrofuran crystallised in the same space group *C*2 and was therefore not fully characterised. It is of interest to note that Karrer and co-worker mentioned that **4** could not be obtained in a crystalline state.[14]

a) 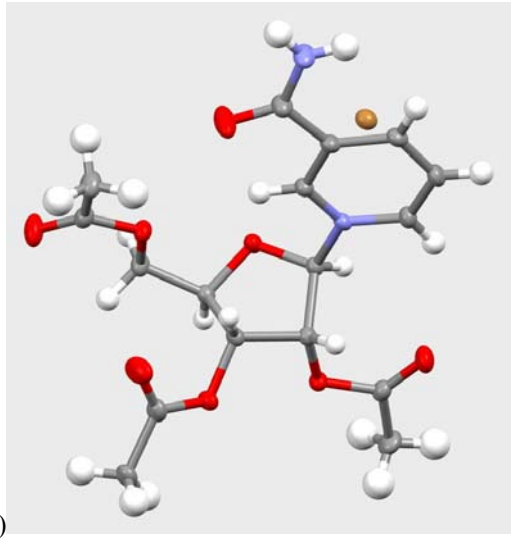 b) 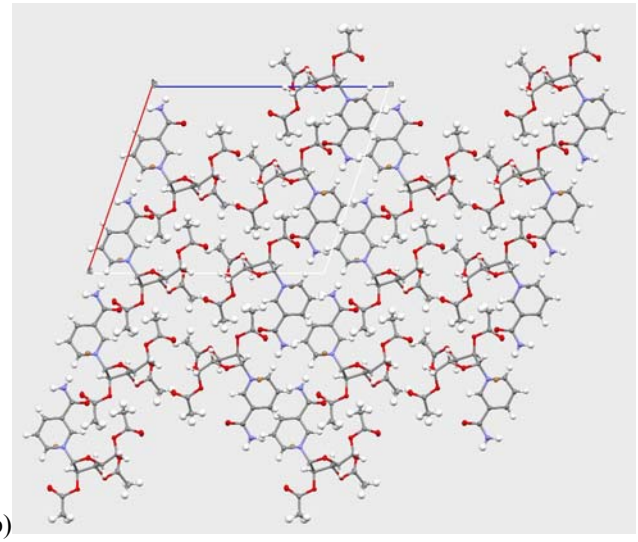

Figure 7: a) Displacement ellipsoid representation of **4**, ellipsoids drawn at 50% probability. b) packing diagram of **4**.

In 2018, two groups from the Queen's University of Belfast and the ChromaDex company published a patent application, in which they showed the powder X-ray pattern of nicotinamide-β-D-riboside triacetate chloride (Figure 8).[15] We took the coordinates of the corresponding bromide salt (**4**) and artificially substituted the bromide by a chloride ion. Without any further optimisation, we used these coordinates to simulate the X-ray the PXRD pattern of nicotinamide-β-D-riboside triacetate chloride (Figure 9). As one sees, the powder pattern is rather similar with the experimental one displayed in Figure 8, indicating that the chloride salt described in patent application US20180134743A1 and the bromide of nicotinamide-β-D-riboside triacetate presented in this work are isostructural.

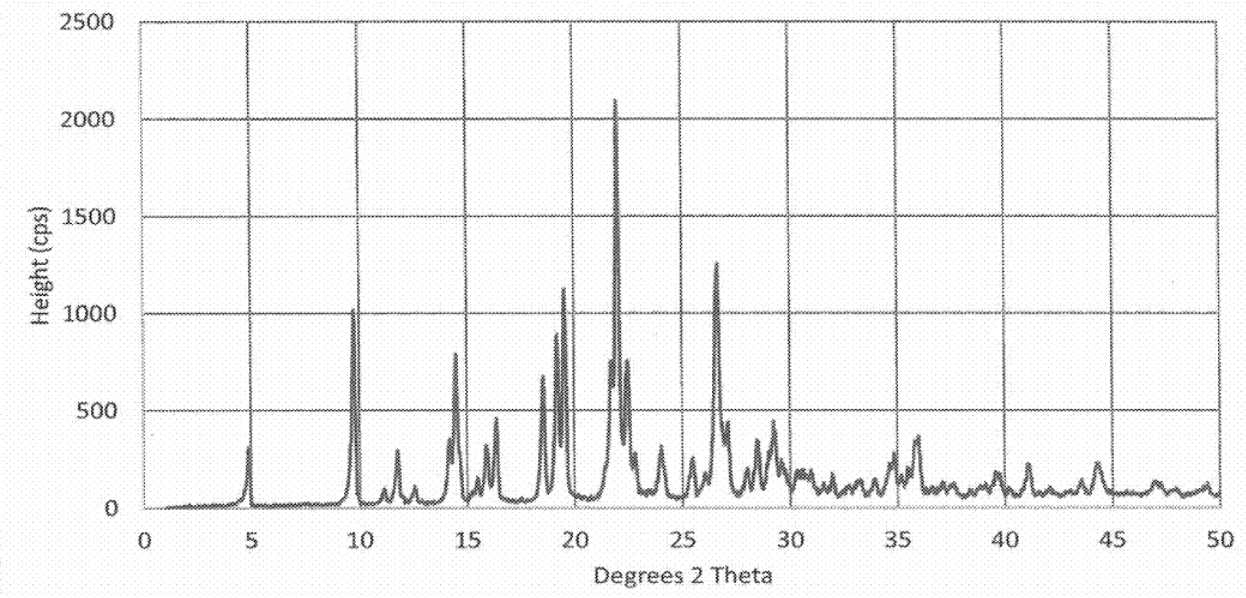

Figure 8: Published PXRD pattern of nicotinamide-β-D-riboside triacetate chloride from the patent application US20180134743A1.[15]

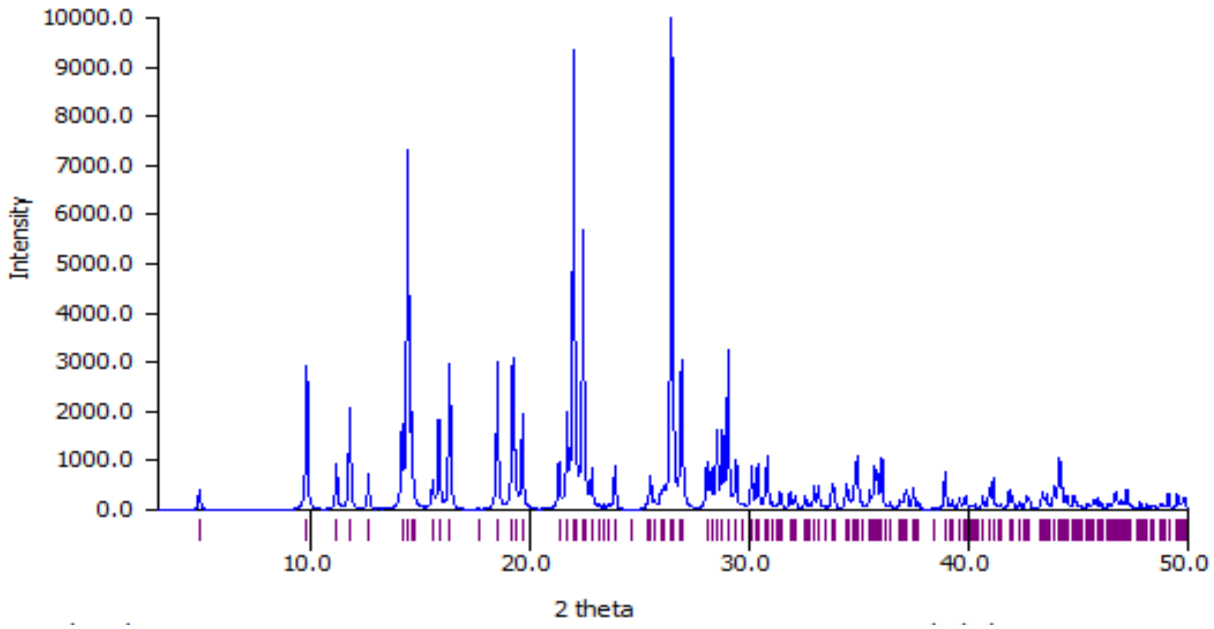

Figure 9: Simulated PXRD pattern of nicotinamide-β-D-riboside triacetate chloride, taking the coordinates of the corresponding bromide salt (**4**) and substituting the bromide by a chloride ion.

2.5 Thionicotinamide-β-D-riboside triacetate bromide (5)

Single crystals were obtained by vapour diffusion at 23°C of 4 mg of **5** dissolved in methanol against a reservoir of tetrahydrofuran. The crystallographic data is summarised in Table 2. **5** crystallised in the triclinic, chiral space group *P*1. The asymmetric unit consists of two molecules of **5** (Figure 10). The

two molecules in the asymmetric unit possess almost the same configuration (see Figure S1 for an overlay of the two structures). The absolute configuration of the enantiomerically pure molecule was confirmed by the Flack parameter (-0.004(9)) and by comparison with the expected stereochemistry. The crystals are non-merohedral twins (ratio of 52:48) with the unit cells in the two different domains rotated by 180° perpendicular to the *bc* plane (Figure S2). The nitrogen of the amide group forms two hydrogen bonds to a bromide (N2-H2A Br21(1+x, 1+y, 1+z): 3.403(5) Å, N2-H2B Br1(x, 1+y, z): 3.365(5) Å, N22-H22A Br1(-1+x, -1+y, -1+z): 3.403(5) Å, N22-H22B Br21(x, -1+y, z): 3.365(5) Å).

a)

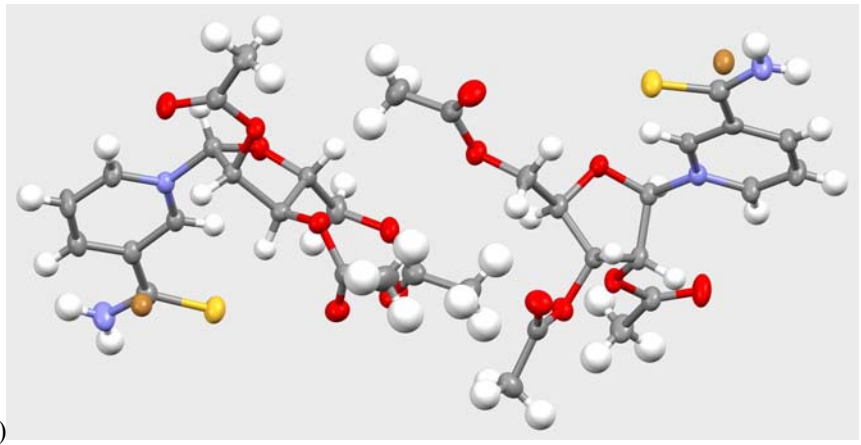

b)

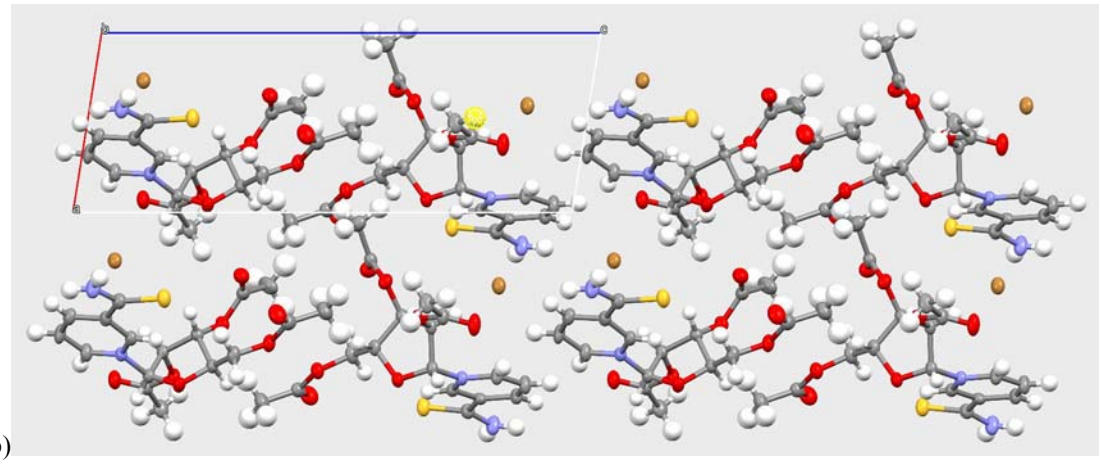

Figure 10: a) Displacement ellipsoid representation of **5**, ellipsoids drawn at 50% probability.
b) packing diagram of **5**.

Table 2: Summary of crystal data and structure refinement of **4** and **5**.

	4	**5**
Empirical formula	$[C_{17}H_{21}N_2O_8][Br]$	$[C_{17}H_{21}N_2O_7S][Br]$
mol. weight [g/mol]	461.27	477.33
Crystal system	monoclinic	triclinic
Space group	*C*2	*P*1
a [Å]	15.9437(4)	7.02352(12)
b [Å]	6.73890(10)	8.61252(13)
c [Å]	19.1317(5)	18.1023(2)
α [°]	90	90.2744(10)
β [°]	109.064(3)	98.3915(11)
γ [°]	90	110.7171(14)
Volume [$Å^3$]	1942.83(8)	1011.35(3)
Z	4	2
Density(calc.) [mg/m^3]	1.577	1.567
Abs. coeff. [mm^{-1}]	2.163	4.111
F(000)	944	488
Crystal size [mm^3]	0.227 x 0.187 x 0.055	0.12 x 0.09 x 0.012
Crystal description	colourless plate	yellow plate
Θ range [°]	2.253 to 33.216	4.948 to 78.973
Index ranges	$-22\leq h\leq 24$, $-10\leq k\leq 10$, $-28\leq l\leq 27$	$-8\leq h\leq 8$, $-10\leq k\leq 10$, $-23\leq l\leq 23$
Reflections collected	32123	14545
Indep. reflections	6693 [R_{int} = 0.0244]	14545
Reflections obs.	6367	14370
Criterion for obs.	$I > 2\sigma(I)$	$I > 2\sigma(I)$
Completeness to Θ [°]	99.9% to 25.242	94.9% to 67.684
Absorption correction	semi-empirical from equivalents	semi-empirical from equivalents
Max. and min. transmission	1.000 and 0.512	1.00000 and 0.90407
Data / restraints / parameters	6693 / 1 / 256	14545 / 3 / 512
Goodness-of-fit on F^2	1.036	1.040
Final R indices [$I > 2\sigma(I)$]	R_1 = 0.0192, wR_2 = 0.0494	R_1 = 0.0369, wR_2 = 0.0993

R indices (all data)	$R_1 = 0.0211$, $wR_2 = 0.0499$	$R_1 = 0.0373$, $wR_2 = 0.0996$
Flack parameter	-0.0040(17)	-0.004(9)
Final $\Delta\rho_{max,min}$ [$e^-/Å^3$]	0.41 and -0.24	0.93 and -0.31

2.6 Isostructurality

When comparing all structures **1**-**5**, it becomes evident that the chloride and bromide salts of NR (**1** and **2**) and the bromide salt of the corresponding thioamide (**3**) are all isostructural. However, the crystal structures of the triacetate bromide salt (**4**) and its thioamide derivative **5** are non-isostructural. The fact that chloride and bromide salts can form isostructural crystal structures is quite well known, see e.g. references [16,17] for two examples. It remains the question, why the substitution of the carbonyl oxygen with a sulfur atom to yield a thioamide gives raise to an isostructural structure in the case of salt **3** but not for **5**? The nitrogen and the oxygen atom of the amide in the case of **2** are part of an extended hydrogen network as already discussed. Surprisingly, this hydrogen binding pattern remains the same, when the oxygen atom in **2** is substituted by a sulfur atom in **3**, therefore generating the isostructural arrangement. On the other hand, neither the oxygen atom of the amide **4** nor the sulfur atom of the thioamide **5** are part of any hydrogen bonding. In both cases, both hydrogen atoms of the NH_2 group are involved in a hydrogen bonding to one bromide anion each. These intermolecular interactions seem to allow different packing types in the cases of **4** and **5**, making their structures non-isostructural.

2.7 Torsion angle χ of the nicotinamide riboside derivatives

For all NR derivatives characterised above, the torsion angle χ was measured and their values are summarised in Table 3. For comparison, the only two other nicotinamide ribosides with comparable structures (Figure 11) were chosen from the Cambridge Structural Database, lithium (5'-nicotinamide-ribosyl)-(5'-adenyl)-pyrophosphate dihydrate ($Li(NAD)\cdot(H_2O)_2$, **6**)[18] and (5'-nicotinamide-ribosyl)-(5'-adenyl)-pyrophosphate tetrahydrate ($H(NAD)\cdot(H_2O)_4$, **7**)[19], in which the adenine is protonated. They crystallise in different space groups and have different torsion angles as listed in Table 3.

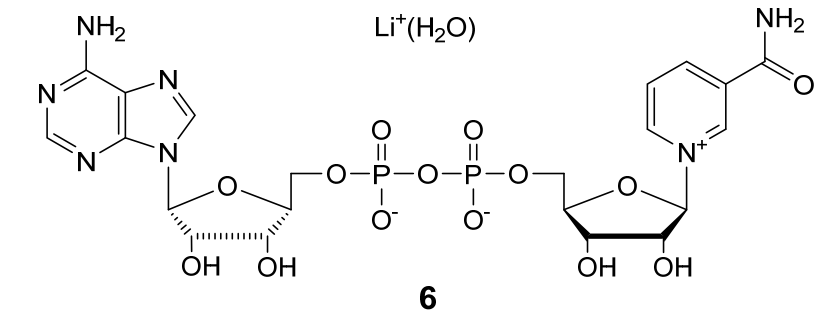

6

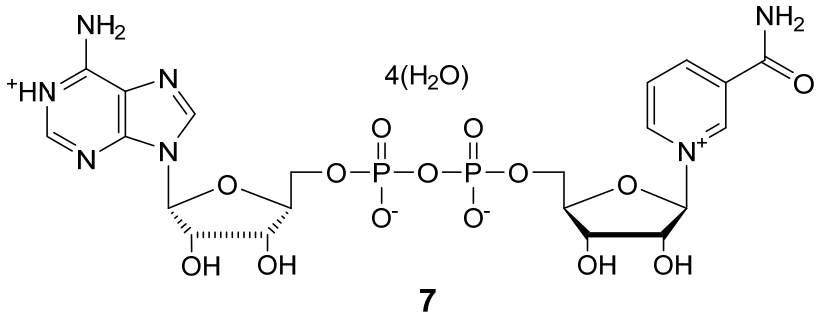

7

Figure 11: Structures of **6** and **7**.

Table 3: Torsion angle χ of different NR derivatives.

NR	torsion angle [°]	conformation	space group	Reference
1	-136.09(15)	*anti*	$P2_12_12_1$	This work
2	-137.1(2)	*anti*	$P2_12_12_1$	This work
3	-137.8(2)	*anti*	$P2_12_12_1$	This work
4	26.2(2)	*syn*	$C2$	This work
5	10.6(8)	*syn*	$P1$	This work
6	-165.42	*anti*	$P2_12_12_1$	[18]
7	-150.32(9)	*anti*	$P1$	[19]
protein structures containing nicotinamide riboside**:**				
PDB 2QT0	5.8	*syn*		[20]
PDB 2QT1	-2.9	*syn*		[20]
PDB 4QTN	6.4	*syn*		[21]

The nicotinamide ribosides and their derivatives listed in Table 3 can be divided in two groups. The nicotinamide ribosides **1**-**3** with alcohol groups at the riboside and the two NAD structures **6** and **7** have a χ torsion angle of -135° to -165°. This corresponds to the nicotinamide being in the *anti* position. In

contrast, the torsion angles of the nicotinamide ribosides with triacetate groups **4** and **5** are between 10° and 30°, which corresponds to the nicotinamide unit being in the *syn* position. There are 3 protein structures containing also a nicotinamide riboside cation, in all these 3 cases the nicotinamide is in the *syn* conformation. The group of Eisenberg discussed the χ torsion angles of NAD in oxidoreductase enzymes co-structures and found that the torsion angles were in the *syn* and the *anti* conformation.[22] The current version of the pdb database[23] contains more than 1300 protein structures that co-crystallized with a NAD.

3. Conclusion

For the first time, the X-ray structures of nicotinamide riboside salts could be determined. All nicotinamide riboside derivatives (**1**-**5**) were successfully crystallised by the vapour diffusion method. In contrast, the crystallization setups with the layering technique led to the decomposition of the nicotinamide ribosides, because of the slow process of crystallization compared to the vapour diffusion. The obtained single crystals were measured on a Synergy diffractometer at 160 K and for each one of the compounds **1**-**5** the crystal structure could be determined. The 3 structures of nicotinamide-β-D-riboside chloride (**1**), nicotinamide-β-D-riboside bromide (**2**) and thionicotinamide-β-D-riboside bromide (**3**) are isostructural. The χ torsion angles of the five nicotinamide riboside derivatives were compared with those obtained from the two NAD crystal and the three protein nicotinamide riboside co-crystal structures.

4. Experimental

Nicotinamide-β-D-riboside chloride (**1**), nicotinamide-β-D-riboside bromide (**2**)[24], thionicotinamide-β-D-riboside bromide (**3**), nicotinamide-β-D-riboside triacetate bromide (**4**)[24,25], and thionicotinamide-β-D-riboside triacetate bromide (**5**) were provided by *Biosynth AG*. Tetrahydropyran (≥99%) was purchased from *Fluka*. Methanol (≥99.9%), ethanol (≥99.9%), acetone (≥99.9%), acetonitrile (≥99.9%), chloroform (≥99%), cyclohexane (≥99.5%), tetrahydrofuran (THF, ≥99.9%) were purchased from *Sigma Aldrich*. All chemicals were used without further purification.

4.1 Nicotinamide riboside derivatives

All nicotinamide riboside derivatives were crystallised using the vapour diffusion technique.[11] For each 4 mg of nicotinamide riboside was dissolved in about 1 ml of solvent in the inner tube as listed

in Table 4. Not dissolved particles were filtered off. The inner tube was then placed in the outer container. About 3 ml of antisolvent was added into the outer container and the container was then closed. The used solvents, antisolvents and the results are listed in Table 4. When crystals were observed the container was opened and the crystal removed for x-ray single crystal diffraction measurement. Exemplary crystals for each of the NR derivatives are shown in Figure 12.

Table 4: Summary of vapour diffusion setups for the NR derivatives.

NR	Solvent	Antisolvent	result
1	Methanol	Tetrahydrofuran	white clots, bad crystals
1	Acetone	Chloroform	no crystals
1	Acetonitrile	Tetrahydropyran	no crystals
1	Ethanol	Cyclohexane	crystals
2	Methanol	Tetrahydrofuran	crystals
3	Methanol	Tetrahydrofuran	crystals
4	Methanol	Tetrahydrofuran	crystals
4	Ethanol	Cyclohexane	crystals
5	Methanol	Tetrahydrofuran	bad needles
5	Ethanol	Cyclohexane	twinned crystal

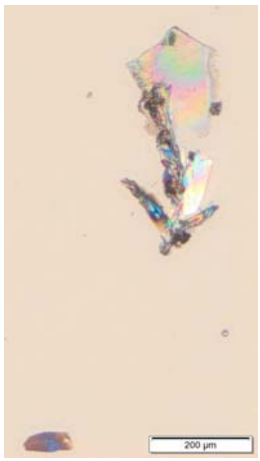

(a)

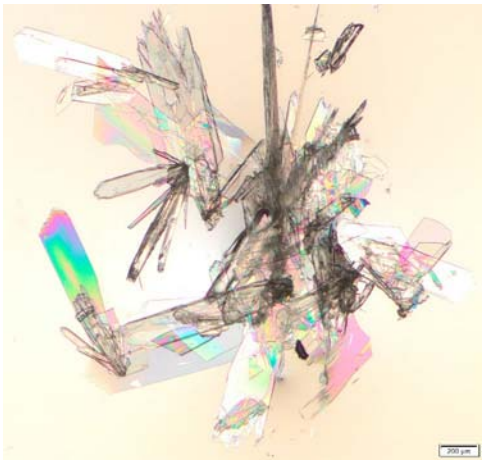

(b)

(c)

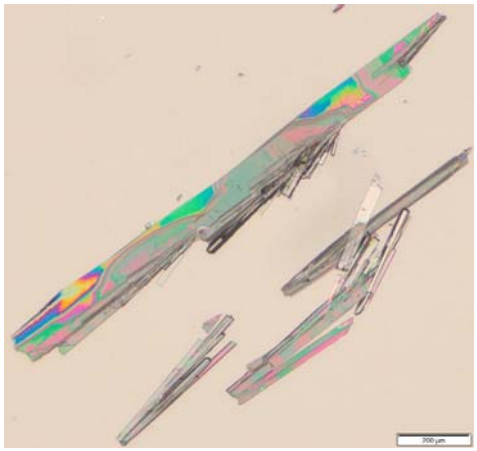

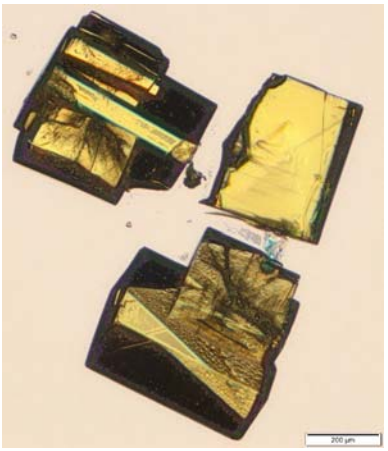

(d) (e)

Figure 12: Photos of the grown crystals of (a) **1**, (b) **2**, (c) **3**, (d) **4**, (e) **5**. All scale bars are 200 μm.

4.2 X-ray Single Crystal Diffusion

Crystallographic data were collected at 160.0(1) K on a Rigaku-Oxford Diffraction XtaLAB Synergy-S dual source diffractometer. This is a kappa-axis four-circle goniometer with a Dectris Pilatus3 R 200K HPC (Hybrid Photon Counting) detector and Cu (for **1**, **3**, and **5**) and Mo (for **2** and **4**) PhotonJet microfocus X-ray sources. Suitable crystals were covered with oil (Infineum V8512, formerly known as Paratone N), placed on a nylon loop that is mounted in a CrystalCap Magnetic™ (Hampton Research) and immediately transferred to the diffractometer. The program suite *CrysAlisPro* was used for data collection, absorption correction and data reduction.[26] The structures were solved with the dual-space algorithm using *SHELXT*[27] and were refined by full-matrix least-squares methods on F^2 with *SHELXL-2014*[28] using the GUI *Olex2*[29]. The graphical output and the simulation of the X-ray powder patterns was generated with the help of the program *Mercury*.[30] CCDC 1903825-1903829 contain the supplementary crystallographic data for this paper. The data can be obtained free of charge from The Cambridge Crystallographic Data Centre via www.ccdc.cam.ac.uk/structures.

Supporting Information

The Supporting Information is available free of charge on the ACS Publications website at DOI: 10.1021/acs.cgd.YYYYYY. Overlay of the two molecules in the asymmetric unit of **5** and orientation of the two non-merohedral twinning components in the crystal of **5**. (PDF)

Notes

Günter Schabert, Aysel Soydemir, Lukas Wick and Urs Spitz are employees of Biosynth, a firm that sells various nicotinamide riboside derivatives.

Acknowledgements

We thank the University of Zurich and the R'Equip programme of the Swiss National Science Foundation (project No. 206021_164018) for financial support.

References

(1) Ratajczak, J.; Joffraud, M.; Trammell, S. A. J.; Ras, R.; Canela, N.; Boutant, M.; Kulkarni, S. S.; Rodrigues, M.; Redpath, P.; Migaud, M. E.; Auwerx, J.; Yanes, O.; Brenner, C.; Canto, C. NRK1 controls nicotinamide mononucleotide and nicotinamide riboside metabolism in mammalian cells. *Nat. Commun.* **2016**, *7*, 13103.

(2) Zhang, H.; Ryu, D.; Wu, Y.; Gariani, K.; Wang, X.; Luan, P.; D'Amico, D.; Ropelle, E. R.; Lutolf, M. P.; Aebersold, R.; Schoonjans, K.; Menzies, K. J.; Auwerx, J. NAD^+ repletion improves mitochondrial and stem cell function and enhances life span in mice. *Science* **2016**, *352*, 1436-1443.

(3) Makarov, M. V.; Migaud, M. E. Syntheses and chemical properties of β-nicotinamide riboside and its analogues and derivatives. *Beilstein J. Org. Chem.* **2019**, *15*, 401-430.

(4) Chi, Y.; Sauve, A. A. Nicotinamide riboside, a trace nutrient in foods, is a Vitamin B3 with effects on energy metabolism and neuroprotection. *Curr. Opin. Clin. Nutr. Metab. Care* **2013**, *16*, 657-661.

(5) Bieganowski, P.; Brenner, C. Discoveries of nicotinamide riboside as a nutrient and conserved *NRK* genes establish a Preiss-Handler independent route to NAD^+ in fungi and humans. *Cell* **2004**, *117*, 495-502.

(6) Yang, T.; Chan, N. Y.-K.; Sauve, A. A. Syntheses of nicotinamide riboside and derivatives: Effective agents for increasing nicotinamide adenine dinucleotide concentrations in mammalian cells. *J. Med. Chem.* **2007**, *50*, 6458-6461.

(7) U.S. Food and Drug Administration (U.S. FDA), Center for Food Safety and Applied Nutrition (CFSAN), Office of Food Additive Safety. GRN 635. Generally recognized as safe (GRAS) determination for Niagen™ (Nicotinamide Riboside Chloride). **2016**, https://www.fda.gov/downloads/Food/GRAS/ucm505226.pdf, accessed on 14.03.2019.

(8) Martens, C. R.; Denman, B. A.; Mazzo, M. R.; Armstrong, M. L.; Reisdorph, N.; McQueen, M. B.; Chonchol, M.; Seals, D. R. Chronic nicotinamide riboside supplementation is well-tolerated and elevates NAD^+ in healthy middle-aged and older adults. *Nat. Commun.* **2018**, *9*, 1286.

(9) Trammell, S. A. J.; Yu, L. P.; Redpath, P.; Migaud, M. E.; Brenner, C. Nicotinamide Riboside Is a Major NAD^+ Precursor Vitamin in Cow Milk. *J. Nutr.* **2016**, *146*, 957-963.

(10) Carlson, E. C.; Standen, M. C.; Morrill, W. M.; W.R. Grace & Co., USA: WO2016014927A2, 2016, p 37.

(11) Spingler, B.; Schnidrig, S.; Todorova, T.; Wild, F. Some thoughts about the single crystal growth of small molecules. *CrystEngComm* **2012**, *14*, 751-757.

(12) Oppenheimer, N. J. NAD hydrolysis: chemical and enzymatic mechanisms. *Mol. Cell. Biochem.* **1994**, *138*, 245-251.

(13) Szczepankiewicz, B.; Koppetsch, K.; Perni, R. B.; GlaxoSmithKline Intellectual Property No.2 Limited, UK: WO2015186068A1, 2015, p 106.

(14) Viscontini, M.; Marti, M.; Karrer, P. Preparation of an iso[3-carbamoyl-N^1-D-ribosidopyridinium] and related compounds. *Helv. Chim. Acta* **1954**, *37*, 1373-1378.

(15) Migaud, M. E.; Redpath, P.; Crossey, K.; Cunningham, R.; Erickson, A.; Nygaard, R.; Storjohann, A.; The Queen's University of Belfast, UK; ChromaDex Inc.: US20180134743A1, 2018, p 262.

(16) Cincic, D.; Kaitner, B. Hydrogen bonding in the bromide salts of 4-aminobenzoic acid and 4-aminoacetophenone. *Acta Cryst.* **2008**, *C64*, o226-o229.

(17) de Moraes, L. S.; Kennedy, A. R.; Logan, C. R. Crystal structures of three halide salts of L-asparagine: an isostructural series. *Acta Cryst.* **2018**, *E74*, 1619-1623.

(18) Reddy, B. S.; Saenger, W.; Mühlegger, K.; Weimann, G. Crystal and Molecular-Structure of the Lithium Salt of Nicotinamide Adenine-Dinucleotide Dihydrate (NAD^+, DPN^+, Cozymase, Codehydrase I). *J. Am. Chem. Soc.* **1981**, *103*, 907-914.

(19) Guillot, B.; Jelsch, C.; Lecomte, C. The oxidized form of nicotinamide adenine dinucleotide. *Acta Cryst.* **2000**, *C56*, 726-728.

(20) Tempel, W.; Rabeh, W. M.; Bogan, K. L.; Belenky, P.; Wojcik, M.; Heather, F. S.; Nedyalkova, L.; Yang, T.; Sauve, A. A.; Park, H. W.; Brenner, C. Nicotinamide riboside kinase structures reveal new pathways to NAD^+. *PLoS Biol.* **2007**, *5*, 2220-2230.

(21) Jaehme, M.; Guskov, A.; Slotboom, D. J. Crystal structure of the vitamin B_3 transporter PnuC, a

full-length SWEET homolog. *Nat. Struct. Mol. Biol.* **2014**, *21*, 1013-1015.
(22) Bell, C. E.; Yeates, T. O.; Eisenberg, D. Unusual conformation of nicotinamide adenine dinucleotide (NAD) bound to diphtheria toxin: A comparison with NAD bound to the oxidoreductase enzymes. *Protein Sci.* **1997**, *6*, 2084-2096.
(23) Burley, S. K.; Berman, H. M.; Bhikadiya, C.; Bi, C.; Chen, L.; Di Costanzo, L.; Christie, C.; Dalenberg, K.; Duarte, J. M.; Dutta, S.; Feng, Z.; Ghosh, S.; Goodsell, D. S.; Green, R. K.; Guranovic, V.; Guzenko, D.; Hudson, B. P.; Kalro, T.; Liang, Y.; Lowe, R.; Namkoong, H.; Peisach, E.; Periskova, I.; Prlic, A.; Randle, C.; Rose, A.; Rose, P.; Sala, R.; Sekharan, M.; Shao, C.; Tan, L.; Tao, Y. P.; Valasatava, Y.; Voigt, M.; Westbrook, J.; Woo, J.; Yang, H.; Young, J.; Zhuravleva, M.; Zardecki, C. RCSB Protein Data Bank: biological macromolecular structures enabling research and education in fundamental biology, biomedicine, biotechnology and energy. *Nucleic Acids Res.* **2019**, *47*, D464-D474.
(24) Lee, J.; Churchil, H.; Choi, W. B.; Lynch, J. E.; Roberts, F. E.; Volante, R. P.; Reider, P. J. A chemical synthesis of nicotinamide adenine dinucleotide (NAD^+). *Chem. Commun.* **1999**, 729-730.
(25) Mikhailopulo, I. A.; Pricota, T. I.; Timoshchuk, V. A.; Akhrem, A. A. Synthesis of Glycosides of Nicotinamide and Nicotinamide Mono-Nucleotide. *Synthesis* **1981**, 388-389.
(26) *CrysAlis^{Pro} Software system*; Rigaku Oxford Diffraction, vers. 1.171.39; Rigaku Corporation: Oxford, UK, 2017.
(27) Sheldrick, G. M. SHELXT - Integrated space-group and crystal-structure determination. *Acta Cryst.* **2015**, *A71*, 3-8.
(28) Sheldrick, G. M. Crystal structure refinement with SHELXL. *Acta Cryst.* **2015**, *C71*, 3-8.
(29) Dolomanov, O. V.; Bourhis, L. J.; Gildea, R. J.; Howard, J. A. K.; Puschmann, H. OLEX2: a complete structure solution, refinement and analysis program. *J. Appl. Cryst.* **2009**, *42*, 339-341.
(30) Macrae, C. F.; Bruno, I. J.; Chisholm, J. A.; Edgington, P. R.; McCabe, P.; Pidcock, E.; Rodriguez-Monge, L.; Taylor, R.; van de Streek, J.; Wood, P. A. Mercury CSD 2.0 - new features for the visualization and investigation of crystal structures. *J. Appl. Cryst.* **2008**, *41*, 466-470.

For Table of Contents Use Only

Nicotinamide Riboside Derivatives: Single Crystal Growth and Determination of X-ray Structures

Ricardo Alvarez, Günter Schabert, Aysel Soydemir, Lukas Wick, Urs Spitz, Bernhard Spingler

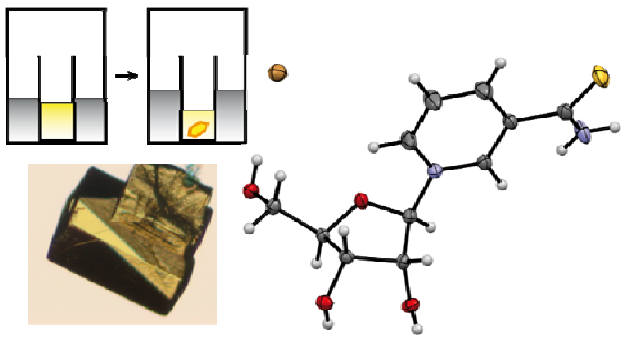

The first single crystal growth of any nicotinamide ribose (NR) salt is reported. Vapour diffusion yielded the crystal structures of five different NR derivatives. The structures are compared with already reported powder patterns.

Supporting information for

Nicotinamide Riboside Derivatives: Single Crystal Growth and Determination of X-ray Structures

Ricardo Alvarez[1], Günter Schabert[2], Aysel Soydemir[2], Lukas Wick[2], Urs Spitz[2], Bernhard Spingler[1*]

[1] Department of Chemistry, University of Zurich, 8057 Zurich, Switzerland

[2] BIOSYNTH AG, Rietlistrasse 4, 9422 Staad, Switzerland

[*] Corresponding author: spingler@chem.uzh.ch

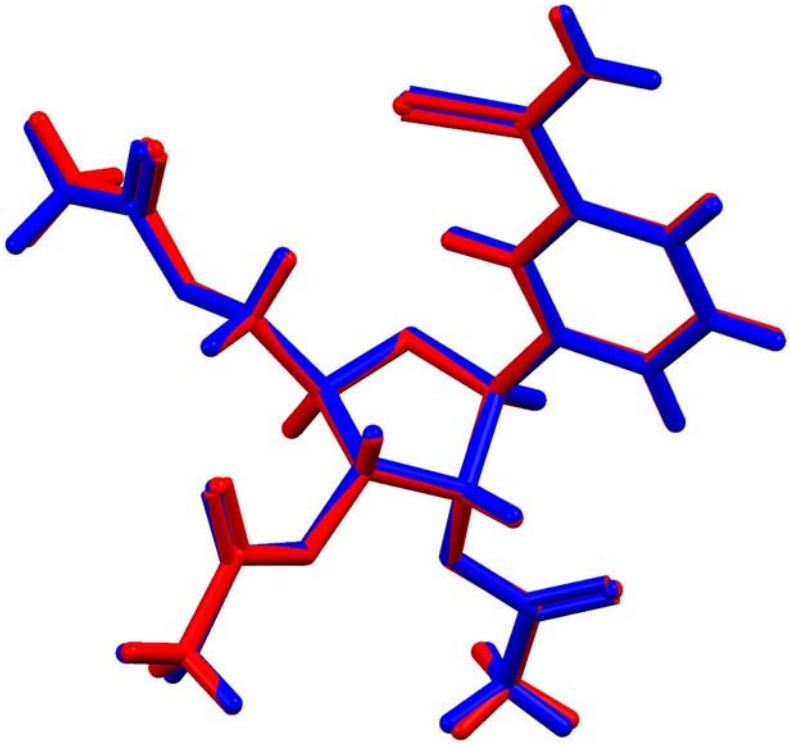

Figure S1: Overlay of the two molecules in the asymmetric unit of **5**.

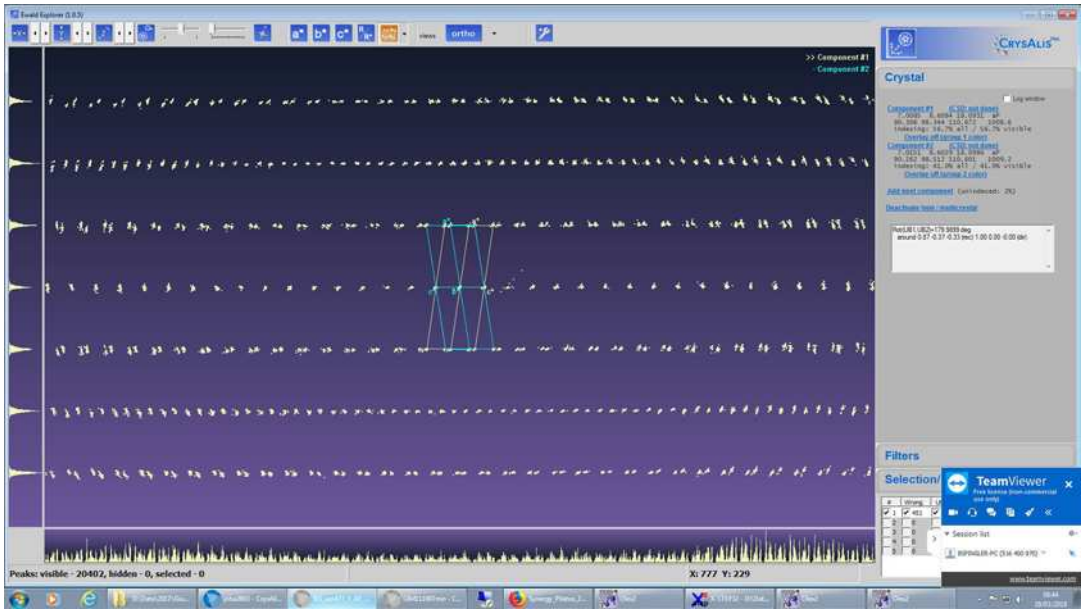

Figure S2: Orientation of the two non-merohedral twinning components in the crystal of **5**.